© 2014. Published by The Company of Biologists Ltd | Journal of Cell Science (2014) 127, 4740–4749 doi:10.1242/jcs.155721

RESEARCH ARTICLE

The lipid-transfer protein Nir2 enhances epithelial-mesenchymal transition and facilitates breast cancer metastasis

Omer Keinan[1,*], Amir Kedan[1,*], Nancy Gavert[1], Michael Selitrennik[1], SoHui Kim[1], Thomas Karn[2], Sven Becker[2] and Sima Lev[1,‡]

ABSTRACT

The involvement of epithelial-mesenchymal transition (EMT) in breast cancer metastasis has been demonstrated in many studies. However, the intracellular proteins and signaling pathways that regulate EMT have not been fully identified. Here, we show that the lipid-transfer protein Nir2 (also known as PITPNM1) enhances EMT in mammary epithelial and breast cancer cells. Nir2 overexpression decreases the expression of epithelial markers and concomitantly increases the expression of mesenchymal markers, whereas silencing of Nir2 expression by small hairpin RNA (shRNA) has opposite effects. Additionally, Nir2 expression is increased during EMT and affects cell morphology, whereas Nir2 depletion attenuates growth factor-induced cell migration. These effects of Nir2 on EMT-associated processes are mainly mediated through the PI3K/AKT and the ERK1/2 pathways. Nir2 depletion also inhibits cell invasion *in vitro* and lung metastasis in animal models. Immunohistochemical analysis of breast cancer tissue samples reveals a correlation between high Nir2 expression and tumor grade, and Kaplan–Meier survival curves correlate Nir2 expression with poor disease outcome. These results suggest that Nir2 not only enhances EMT *in vitro* and breast cancer metastasis in animal models, but also contributes to breast cancer progression in human patients.

KEY WORDS: Nir2, PITPNM1, EMT, Metastasis, Migration, Invasion

INTRODUCTION

Increasing lines of evidence suggest that epithelial-mesenchymal transition (EMT), a crucial developmental process implicated in organ development, tissue repair and organ fibrosis, plays a major role in cancer progression, invasion and metastasis (Xiao and He, 2010). EMT is defined by the loss of epithelial characteristics and the acquisition of a motile, invasive and migratory mesenchymal phenotype (Iwatsuki et al., 2010). This conversion is accompanied by loss of cell–cell adhesion and cell polarity, decrease in the expression of epithelial markers such as E-cadherin, increase in the expression of mesenchymal markers such as vimentin, fibronectin, N-cadherin, alpha-smooth muscle actin (α-SMA), as well as increase in the activity of matrix metalloproteinases (MMPs) (Thiery and Sleeman, 2006). In carcinoma cells, EMT is generally associated with increased aggressiveness, invasion and metastasis, in particular, in the early stages of metastasis (invasion and intravasation), when tumor cells detach from the primary tumor to invade the surrounding stroma and enter the circulation (Savagner, 2001; Thiery, 2002; Gupta and Massagué, 2006).

EMT is a transcriptionally regulated process that is mediated, at least in part, by a number of specific transcription factors including Snai1 and Snai2 (hereafter referred to as Snail1 and Snail2, respectively), ZEB1 and ZEB2, Twist1 and Twist2. Expression of these transcription factors in untransformed epithelial cells efficiently induces EMT (Lee et al., 2006; Savagner, 2010). The activity and expression levels of these transcription factors are controlled by multiple signaling cascades, including the TGFβ signaling pathway, the Wnt, Notch and Hedgehog pathways, as well as several growth factor receptor (GFR) signaling cascades, including the receptors of epidermal growth factor (EGF), insulin-like growth factor 1 (IGF1), fibroblast growth factor (FGF) and hepatocyte growth factor (HGF; also known as MET) (Xiao and He, 2010). The TGFβ pathway, which has been most extensively studied in the context of EMT, cooperates with other signaling cascades including the Wnt, Hedgehog, Notch, Ras–MAPK and the PI3K/AKT pathway to induce EMT (Huber et al., 2005; A. Bellacosa, 2010). The PI3K/AKT pathway is known to play a critical role in human cancer initiation and progression, and is also associated with the induction of EMT (Irie et al., 2005). Expression of activated AKT in epithelial cells causes loss of cell–cell adhesion, loss of apical–basolateral cell polarization, induction of cell motility, and changes in the expression or the distribution of various epithelial and/or mesenchymal markers (Grille et al., 2003).

Recently, we found that the lipid-transfer protein Nir2 (also known as PITPNM1) positively regulates the PI3K/AKT and the MAPK signaling pathways in response to EGF treatment in HeLa and MCF7 cells (Kim et al., 2013). We further showed that Nir2, which contains an N-terminal phosphatidylinositol (PtdIns)-transfer domain (Lev et al., 1999) and mainly localizes at the Golgi complex (Litvak et al., 2005), translocates to the plasma membrane upon stimulation with EGF. At the plasma membrane, Nir2 appears to regulate the PtdIns(4,5)P_2 level and, consequently, the production of PtdIns(3,4,5)P_3, thereby activating the ERK1 and ERK2 (hereafter referred to as ERK1/2), and AKT pathways (Kim et al., 2013). These findings introduced Nir2 as an upstream regulator of the PI3K/AKT and the MAPK signaling pathways, which are activated in response to GFR stimulation.

Here, we show that Nir2 is also an important regulator of cell migration and invasion, and a new modulator of EMT in

[1]Molecular Cell Biology Department, Weizmann Institute of Science, Rehovot 76100, Israel. [2]Department of Obstetrics and Gynecology, Goethe University Frankfurt, Theodor-Stern Kai 7, 60590 Frankfurt, Germany.
*These authors contributed equally to this work.

‡Author for correspondence (sima.lev@weizmann.ac.il)

Received 27 April 2014; Accepted 18 August 2014

Journal of Cell Science

Journal of Cell Science (2014) 127, 4740–4749 doi:10.1242/jcs.155721

mammary epithelial and breast carcinoma cells. We further show that depletion of Nir2 expression inhibits breast cancer metastasis in animal models, and that Nir2 expression correlates with high tumor grade and poor disease outcome in breast cancer patients. These new findings demonstrate the important physiological roles of lipid-transfer proteins, their implication in human diseases, and highlight Nir2 as a potential target for therapeutic intervention.

RESULTS

Depletion of Nir2 expression attenuates the migration of MDA-MB-231 cells

We have previously shown that Nir2 translocates from the Golgi complex to the plasma membrane of HeLa and MCF7 cells in response to EGF treatment (Kim et al., 2013). More recently we observed that Nir2 is expressed in many human breast carcinomas, including MDA-MB-231, T47D and SKBR3 (supplementary material Fig. S1A). Furthermore, several growth factors such as EGF, neuregulin 1 (NRG1) and insulin-like growth factor 1 (IGF1, hereafter referred to as IGF-I) trigger its translocation from the Golgi complex to the plasma membrane (Fig. 1A; supplementary material Fig. S1B,C). These growth factors also enhance the migration of various breast cancer cell lines including that of the highly invasive MDA-MB-231 line (Price et al., 1999; Bartucci et al., 2001; Tsai et al., 2003). Hence, we examined whether Nir2 affects the migration of MDA-MB-231 cells in response to migratory stimuli. The cells were infected with lentiviruses expressing three different shRNAs of Nir2. Two of them (shRNA number 1 and shRNA number 2) efficiently reduced the expression of Nir2 (Fig. 1B) and were used in all the subsequent experiments. The effect of Nir2 depletion on cell migration was assessed in wound-healing (Fig. 1B,C) and transwell migration assays (Fig. 1D). As shown, Nir2 depletion substantially inhibited wound closure in response to EGF, NRG1 and IGF-I as well as to 10% serum. The migration of Nir2-depleted MDA-MB-231 cells through a transwell chamber was also markedly (~63%) attenuated (Fig. 1D).

Previous studies suggested that the PI3K/AKT pathway mediates the migratory responses of IGF-I and EGF in MDA-MB-231 cells (Price et al., 1999; Bartucci et al., 2001). The MAPK pathway is also involved in EGF-induced MDA-MB-231 cell migration (Harrison et al., 2013). We, therefore, examined the influence of Nir2 depletion on these signaling cascades. As

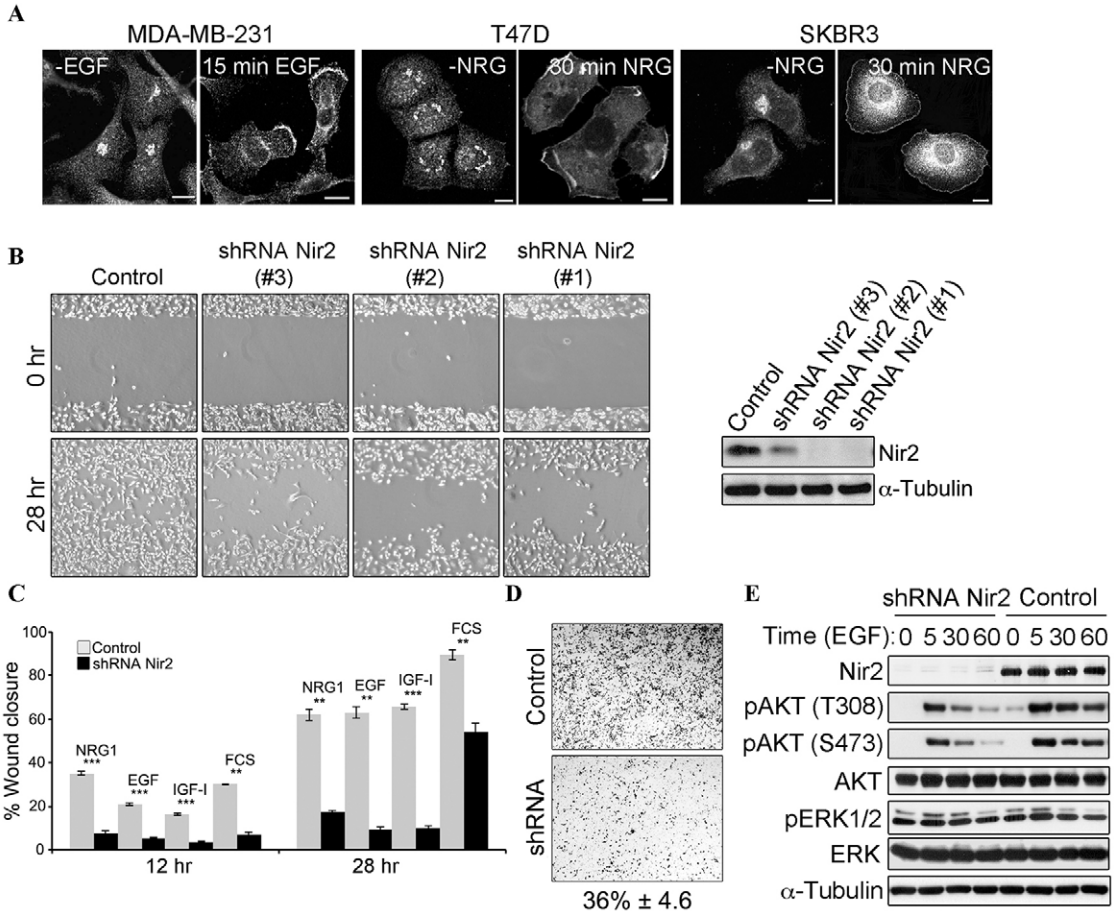

Fig. 1. Depletion of Nir2 affects MDA-MB-231 cell migration and AKT activation. (A) MDA-MB-231, T47D and SKBR3 cells were serum-starved for 24 hr and then stimulated with the indicated growth factors for 15–30 min. The localization of Nir2 was assessed by immunostaining with anti-Nir2 antibody. Staining for p115 was used as a Golgi marker. Shown are representative confocal images. Scale bars: 10 μm. (B-D) Migration of control and Nir2-depleted MDA-MB-231 cells was assessed by wound-healing assay (B,C) or by Boyden chamber assay (D). The effects of three different shRNAs targeting Nir2 on Nir2 protein level and wound closure is shown (B). Wound closure was measured in the presence of the indicated growth factors and calculated as described in Materials and Methods (C). The mean values ±s.d. of four independent experiments are shown. (E) Control and Nir2-depleted MDA-MB-231 cells were serum-starved for 24 hr and then stimulated with EGF (50 ng/ml) for the indicated time periods. Total cell lysates were prepared and analyzed for AKT and ERK1/2 phosphorylation by using the corresponding antibodies and western blot (WB) analysis. Reproducible results were obtained in three independent experiments.

Journal of Cell Science (2014) 127, 4740–4749 doi:10.1242/jcs.155721

shown, depletion of Nir2 markedly reduced the phosphorylation of AKT in response to EGF (Fig. 1E; supplementary material Fig. S1D), consistent with our previous results in HeLa and MCF7 cells (Kim et al., 2013). However, we could not detect any effect on ERK1/2 phosphorylation, possibly owing to the activating mutations within the B-Raf proto-oncogene (BRAF) and the Kirsten rat sarcoma viral oncogene homolog (KRAS) in this specific cell line (Hollestelle et al., 2007). These results suggest that Nir2 regulates the migration of MDA-MB-231 cells mainly through the PI3K/AKT pathway.

Nir2 enhances growth-factor-induced migration of MCF10A cells

Although reduction of Nir2 expression in MDA-MB-231 cells markedly attenuated cell migration, Nir2 overexpression had no obvious effects on the migratory response of these highly motile cells. Nonetheless, overexpression of Nir2 in either the human breast carcinoma cell line T47D or the non-transformed human mammary cell line MCF10A enhanced (approximately twofold) NRG1- or EGF-induced cell migration, respectively (supplementary material Fig. S2A,B). Nir2 overexpression also enhanced TGFβ-induced migration (Fig. 2C) in MCF10A cells, whereas silencing of Nir2 markedly attenuated collective as well as individual cell migration in response to either TGFβ or EGF, as assessed in wound-healing and transwell migration assays (Fig. 2A-C), respectively. These results suggest that Nir2 plays an important role in the migratory responses of MCF10A cells.

Previous studies suggested that the migratory response to EGF and TGFβ in MCF10A cells are mediated, mainly, through the ERK pathway (Kim et al., 2004; Tarcic et al., 2012). We, therefore, examined the effects of Nir2 on ERK1/2 phosphorylation. As shown, overexpression of Nir2 in MCF10A cells enhanced the phosphorylation of ERK1/2 (Fig. 2D), whereas Nir2 depletion reduced ERK1/2 phosphorylation in response to either EGF or TGFβ (Fig. 2D; supplementary material Fig. S2B), consistent with its stimulatory or inhibitory effects on cell migration, respectively (Fig. 2A–C). Furthermore, inhibition of ERK1/2 phosphorylation by the MEK1/2 inhibitor U0126 (supplementary material Fig. S2C), markedly attenuated the migration of MCF10A cells in response to EGF (by 70%) and TGFβ (by 50%) and, apparently, abolished the stimulatory effect of Nir2 overexpression on MCF10A migration (Fig. 2E), suggesting that Nir2 affects the migration of MCF10A cells primarily through the ERK pathway.

Nir2 positively regulates EMT in mammary cells

The marked effect of Nir2 on TGFβ-mediated responses in MCF10A cells (Fig. 2C-E) led us to examine its involvement in EMT, because TGFβ is a potent inducer of EMT (Tumbarello and Turner, 2007). We first examined the effects of TGFβ and EGF, two known EMT inducers of mammary cells (Hardy et al., 2010; Imamura et al., 2012), on the protein and mRNA expression levels of Nir2. TGFβ induces EMT in MCF10A cells (Tumbarello and Turner, 2007) and enhances the mesenchymal properties of MDA-MB-231 cells (Romagnoli et al., 2012), whereas EGF induces EMT in the human breast cancer cell line MDA-MB-468 (Lo et al., 2007). As shown in Fig. 3A, both TGFβ and EGF increased the levels of Nir2 protein in MCF10A, MDA-MB-231 and MDA-MB-468 cells. These elevated levels of Nir2 protein were accompanied by an increase in fibronectin or a decrease in E-cadherin levels, characteristic markers of mesenchymal and epithelial cells, respectively. TGFβ and EGF also enhanced the mRNA levels of Nir2 (Fig. 3B), suggesting that Nir2 is transcriptionally regulated during EMT.

Next, we asked whether Nir2 affects the mesenchymal or epithelial properties of these mammary cell lines. Lentiviruses encoding Nir2-Myc or shRNA targeting Nir2 were used to infect MCF10A, MDA-MB-231 and MDA-MB-468 cells. The effect of Nir2 overexpression or its downregulation on the level of mesenchymal (fibronectin, vimentin, CD44) and epithelial (E-cadherin, ZO-1) protein markers was assessed by western blotting. As shown, overexpression of Nir2 increased the level of mesenchymal markers or decreased the level of epithelial markers, whereas downregulation of Nir2 had opposite effects (Fig. 3C,E; supplementary material Fig. S3A,B). In MCF10A cells, Nir2 overexpression markedly decreased the levels of the tight-junction protein ZO-1 and, consequently, disrupted the integrity of cell–cell contacts as shown by immunostaining of the tight-junction protein ZO-1 and the adherens-junction protein E-cadherin (Fig. 3D). Furthermore, Nir2 expression affected EGF- and TGFβ-induced EMT markers in MDA-MB-468 (Fig. 3F) and in MCF10A cells (Fig. 3G; supplementary material Fig. S3C), respectively. Collectively these results suggest that Nir2 positively regulates EMT.

Downregulation of E-cadherin expression is a hallmark of EMT, and is regulated by specific transcription factors including Snail1 and Snail2, Twist1 and Twist2, ZEB1 and ZEB2 and E47 (TCF3) (Batlle et al., 2000; Bolós et al., 2003). These factors are involved in most physiological EMT processes, and their overexpression in epithelial cell lines often induces EMT (Savagner, 2010). We, therefore, examined the influence of Nir2 on the expression levels of these transcription factors using RT-PCR. Depletion of Nir2 expression in MDA-MB-231 cells by two different shRNAs substantially reduced the expression of Snail1 and ZEB1 and concomitantly increased the expression level of E-cadherin (Fig. 3H), whereas overexpression of Nir2 in MCF10A cells enhanced the expression of Snail1, Twist1, Twist2 and ZEB2 (Fig. 3I). Importantly, expression of the wild-type Nir2 (Nir2-Myc) in Nir2-depleted MDA-MB-231 cells restored the expression levels of Snail1 and ZEB1, thus demonstrating the specificity of the shRNAs effects (Fig. 3H). Furthermore, expression of a myristoylated (constitutively active) form of AKT (Myr-AKT) also restored the expression of vimentin and CD44 in Nir2-depleted MDA-MB-231 and MCF10A cells (Fig. 4A,B). These results suggest that the PI3K/AKT pathway plays a central role in Nir2-enhanced EMT, consistent with the stimulatory effect of Nir2 on this pathway (Figs 1E, 2D).

Nir2 affects cell morphology and invasion

The marked effects of Nir2 on the expression levels of EMT markers (Fig. 3), suggest that Nir2 influences EMT-related cellular processes including cell shape, migration and invasion. Indeed, silencing of Nir2 in MDA-MB-231 cells, which display mesenchymal cell morphology, induced morphological changes characteristic of epithelial cells (Fig. 5A); the cells lost their spindle-like morphology and grew in clusters with established cell–cell contacts. However, overexpression of Nir2 in MCF10A cells, which display epithelial cell morphology, reduced cell–cell contacts and triggered cell scattering (Fig. 5A) – characteristic features of mesenchymal cells.

An additional characteristic feature of EMT is increased invasiveness. We, therefore, examined the influence of Nir2 on the invasion of MCF10A and MDA-MB-231 cells. As shown in Fig. 5B, silencing of Nir2 in either MCF10A or MDA-MB-231

Journal of Cell Science

Journal of Cell Science (2014) 127, 4740–4749 doi:10.1242/jcs.155721

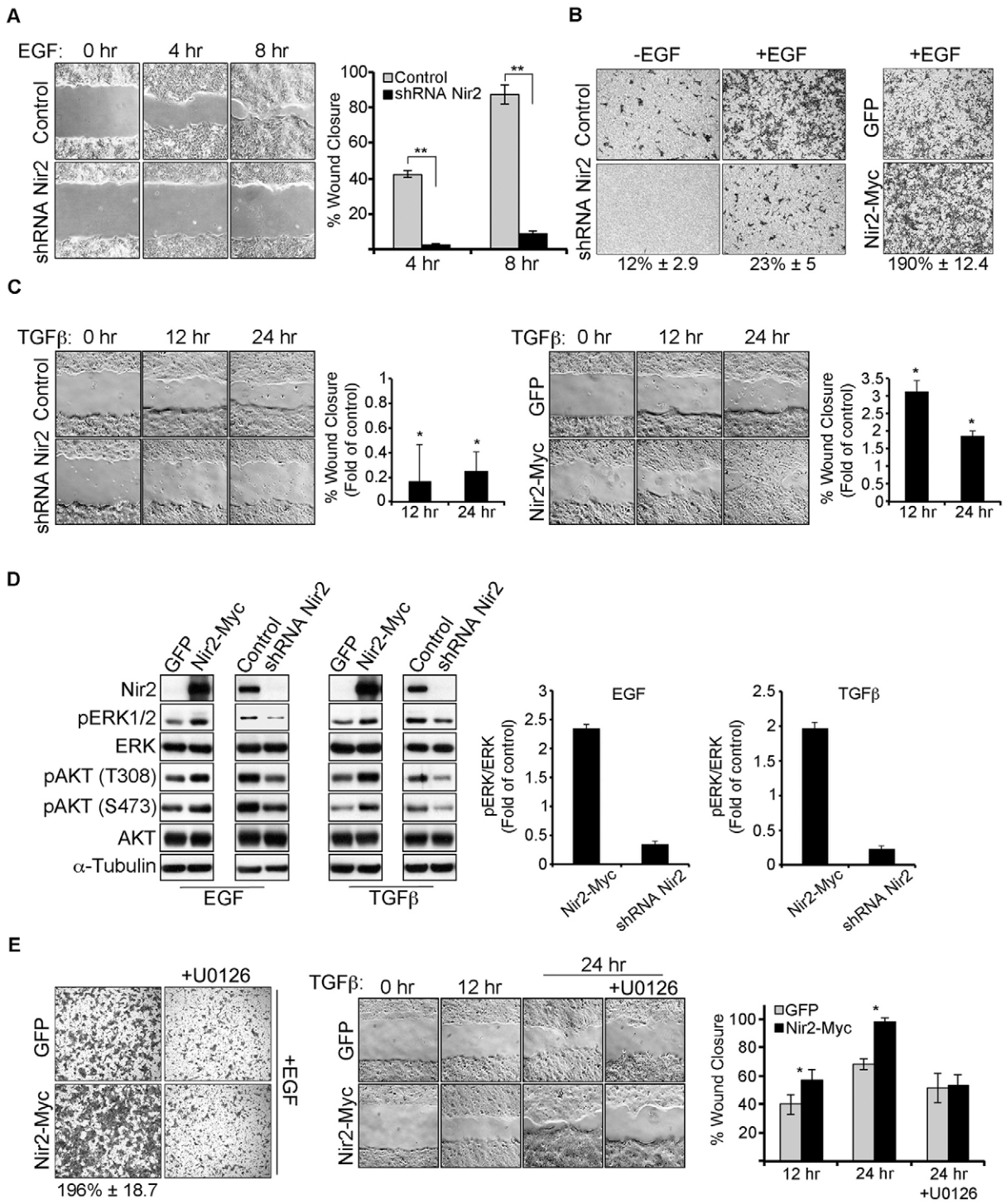

Fig. 2. Nir2 enhances growth-factor-induced cell migration and ERK1/2 activation in MCF10A cells. (A–C,E) Migration of control and Nir2-depleted MCF10A cells in response to EGF treatment (10 ng/ml) or TGFβ (5 ng/ml) was measured either by observing wound closure (A,C,E) or by the Boyden chamber assay (B). The effect of Nir2 overexpression was also assessed by the Boyden chamber assay (B,E). The mean values ±s.d. of four independent experiments are shown in the corresponding graphs. (D) Nir2-depleted or Nir2-overexpressed MCF10A cells were either grown in the presence of EGF or TGFβ for 24 hours. Total cell lysates were prepared and analyzed by western blotting for the indicated proteins. Densitometry analysis was used to estimate the intensity of phosphorylated ERK1/2 (pERK1/2) signals in Nir2-overexpressing or Nir2-depleted MCF10A cells and their corresponding controls. The signal of Nir2-manipulated cells relative to their controls was calculated. The mean values ±s.d. of four independent experiments are shown. (E) Control or Nir2-overexpressing MCF10A cells were grown in the presence of EGF (10 ng/ml) or TGFβ (5 ng/ml) with or without the MEK1/2 inhibitor U0126 (1 μM). Migration was assessed by wound closure or by the Boyden chamber assay. The mean values ±s.d. of three experiments are shown.

Journal of Cell Science (2014) 127, 4740–4749 doi:10.1242/jcs.155721

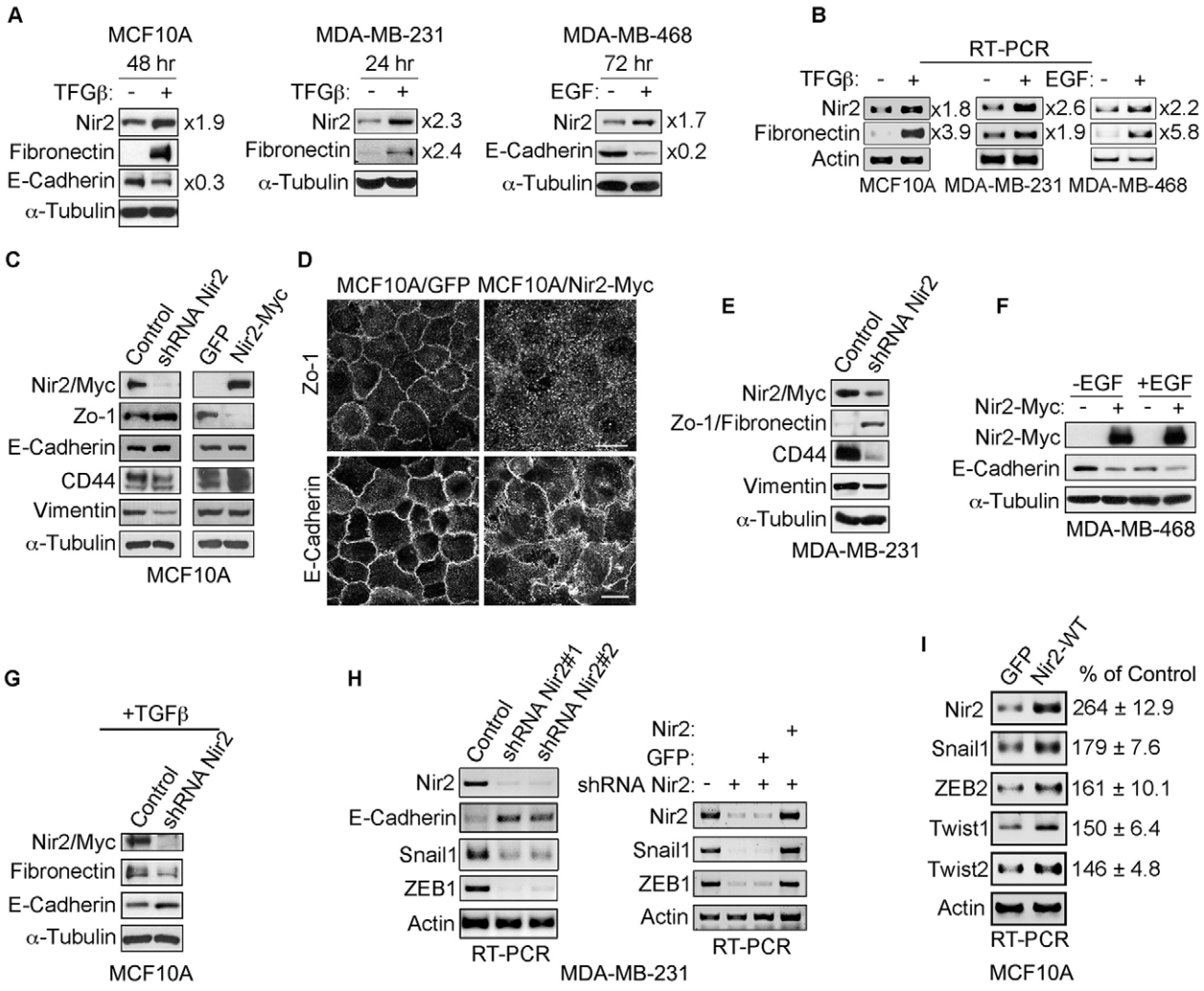

Fig. 3. Nir2 positively regulates EMT in human mammary cell lines. (A,B) MCF10A, MDA-MB-231 and MDA-MB-468 cells were treated with either TGFβ (5 ng/ml) or EGF (10 ng/ml for MCF10A, 50 ng/ml for MDA-MB-468) for the indicated time periods to induce EMT. The protein and mRNA levels of Nir2 as well of indicated cellular markers were assessed by western blotting and RT-PCR, respectively. (C,E,F) The influence of Nir2-overexpression or Nir2 downregulation on the protein levels of the indicated EMT markers was assessed by western blotting using the corresponding antibodies. EMT was induced in MDA-MB-468 by growing the cells in the presence of EGF (50 ng/ml) for 3 days (F). (D) The influence of Nir2-overexpression on cell–cell contact was examined by immunostaining with antibodies against ZO-1 or E-cadherin. Shown are representative confocal images. Scale bars: 10 μm. (G) The influence of Nir2 downregulation on EMT markers induced with TGFβ (5 ng/ml for 3 days) was examined by western blot using the indicated antibodies. (H) The influence of Nir2 depletion in MDA-MB-231 on the mRNA levels of the indicated transcription factors and EMT markers was assessed by RT-PCR. The ability of wild-type Nir2 to restore the level of these transcription factors (right panel) was examined in Nir2-depleted MDA-MB-231 cells by expressing shRNA-resistant Myc-tagged Nir2 (Nir2-Myc). (I) The influence of Nir2 overexpression in MCF10A cells on the mRNA levels of the indicated transcription factors was assessed by using RT-PCR.

cells reduced cell invasion through Matrigel by ~55% or ~63%, respectively. Since matrix metalloproteinases (MMPs) play a major role in cell invasion, we examined the activity of two prominent enzymes; MMP2 and MMP9, in control and Nir2-depleted MCF10A or MDA-MB-231 cells by using the gelatin zymography assay. As shown in Fig. 5C, the activity of MMP2 and MMP9 was significantly reduced in Nir2-depleted cells as compared to control cells. The MMP9 protein level in the conditioned media was also reduced (Fig. 5C), suggesting that Nir2 influences the level of these enzymes rather than their activity. To determine whether Nir2 affects the transcription of these enzymes, we examined the mRNA levels of *MMP2* and *MMP9* as well as of *MMP14* in control and Nir2-depleted MCF10A and MDA-MB-231 cells. As shown, depletion of Nir2 reduced the expression levels of these MMPs (Fig. 5D). Interestingly, previous studies suggest that MMP2, MMP9 and MMP14 are involved in breast cancer progression (Somiari et al., 2006; Têtu et al., 2006; Köhrmann et al., 2009), and that AKT activity promotes *MMP9* transcription in MDA-MB-231 cells (Cho et al., 2008). Hence, the reduced activation of AKT in Nir2-depleted MDA-MB-231 and MCF10A cells (Figs 1E, 2D; supplementary material Figs S1D, S2B), may cause a decrease in *MMP9* transcription. Overall, our results suggest that Nir2 positively regulates EMT and, consequently markedly affects cell morphology and invasion *in vitro*.

Nir2 expression affects lung metastasis in animal models and correlates with poor patient prognosis

The profound effects of Nir2 on cell migration and invasion *in vitro*, led us to examine its influence on breast cancer metastasis

Journal of Cell Science (2014) 127, 4740–4749 doi:10.1242/jcs.155721

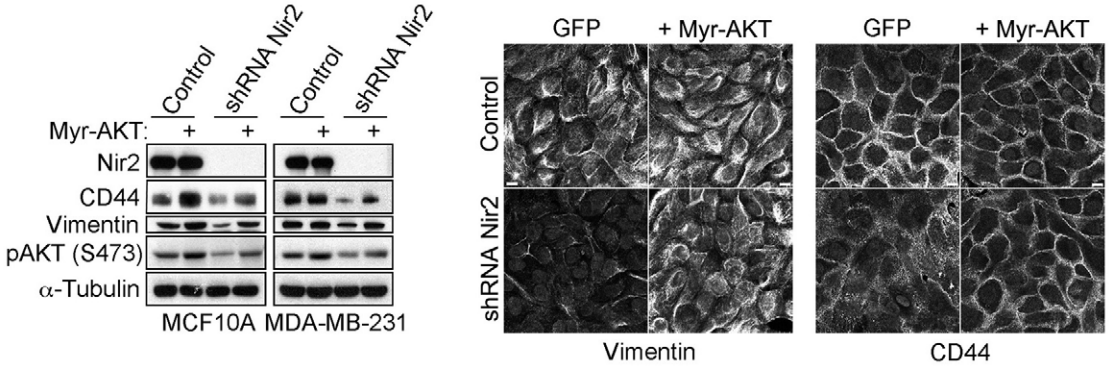

Fig. 4. Constitutively active AKT restores the effect of Nir2 depletion on CD44 and vimentin expression. (A) The influence of constitutively active AKT (Myr-AKT) on the protein expression levels of CD44 and vimentin in control and Nir2-depleted MCF10A and MDA-MB-231 cells was assessed by western blot analysis. (B) The distribution of CD44 and vimentin in the control and Nir2-depleted MCF10A in the absence (GFP) or presence of Myr-AKT is shown in confocal images. Scale bars: 10 μm.

in vivo. MDA-MB-231 cells, which are commonly used in experimental metastasis models, form tumors in the lungs and other organs after tail vein injection. Control and Nir2-depleted MDA-MB-231 cells were injected intravenously into the lateral tail vein of 5-week-old SCID mice. The mice were sacrificed 10 weeks later, the lungs were removed, and the number of metastatic foci on the surface of the lungs was assessed. As shown in Fig. 6A, control MDA-MB-231 cells produced large and numerous metastatic foci (~200 lung metastases/mouse). Depletion of Nir2, however, markedly reduced the number of lung metastases (~20 lung metastases/mouse) (Fig. 6B), and only few micrometastases were detected following H&E staining of lung sections (Fig. 6C). This profound reduction in the number of both metastatic and micrometastatic lesions suggests that loss of Nir2 mainly affects the formation of metastatic foci. It could be, however, that Nir2 also slightly affects metastatic outgrowth as it inhibits the proliferation of the cells by ~28% (supplementary material Fig. S3D).

The striking effect of Nir2 depletion on lung metastasis in animal models led us to hypothesize that the expression levels of Nir2 correlate with poor patient prognosis. To explore this possibility, we used the expression data of 1693 breast cancer patients that had been described by Curtis et al., (Curtis et al., 2012) and found that breast cancer patients who showed high Nir2 expression had a poorer survival rate than patients with low expression (Fig. 7A). Furthermore, immunohistochemistry analysis of paraffin-embedded sections of human breast tissue samples revealed that all samples from healthy individuals had no or a very weak staining for Nir2, whereas the majority (43/56) of cancer samples had moderate to strong Nir2 staining (Fig. 7B,C). Remarkably, positive Nir2 staining was observed in 91% of high-grade tumors, whereas only 64% of low- to intermediate-grade

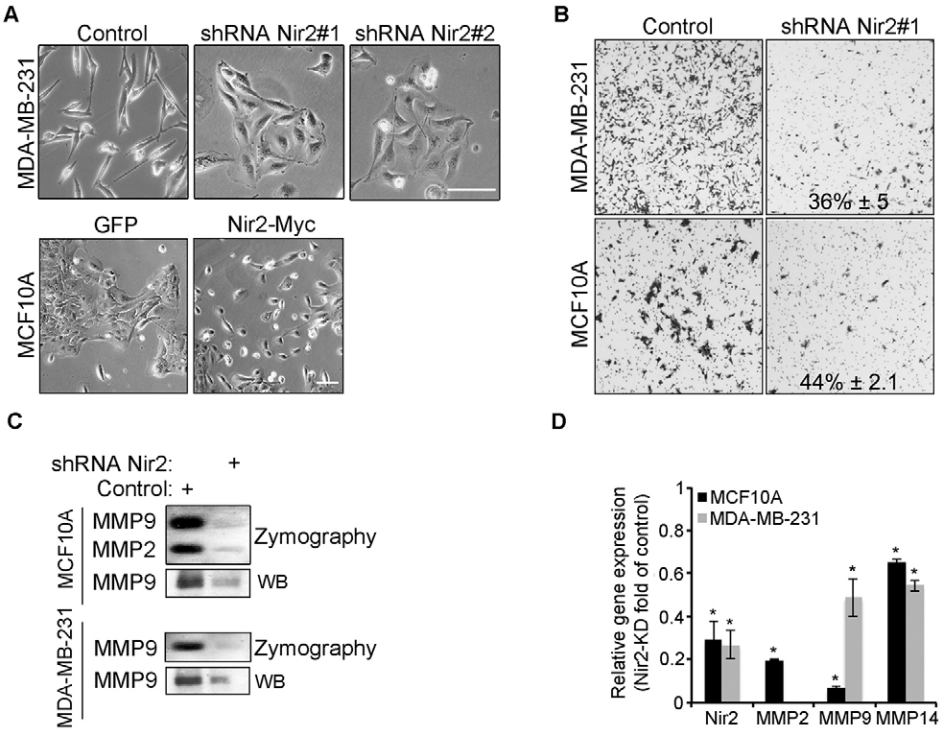

Fig. 5. Nir2 regulates the expression of MMPs as well as cell invasion *in vitro*. (A) Representative phase-contrast images of Nir2-depleted MDA-MB-231 cells and Nir2-overexpressing MCF10A cells. Scale bars: 100 μm. (B) The influence of Nir2 depletion on the invasion of MDA-MB-231 and MCF10A cells through matrigel was assessed by the Boyden chamber assay. Invasion of MCF10A cells was examined in the presence of EGF (10 ng/ml), invasion of MDA-MB-231 cells in the presence of 10% FCS. (C) The activity of MMP2 and MMP9 in control and Nir2-depleted MDA-MB-231 or MCF10A cells was examined by gelatin zymography assay. The activity was assessed in the conditioned cell medium after 16 hrs of incubation in serum-free medium. MMP9 protein level was assessed by western blotting as indicated. (D) The mRNA levels of the indicated MMPs in the control and Nir2-depleted MDA-MB-231 or MCF10A cells were assessed by real-time PCR. Reproducible results were obtained in three independent experiments. The mean values ±s.d. of three experiments are shown; *$P<0.05$.

Journal of Cell Science

Journal of Cell Science (2014) 127, 4740–4749 doi:10.1242/jcs.155721

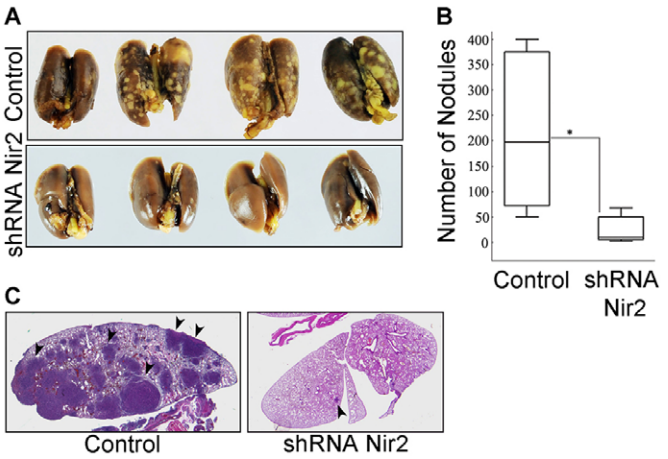

Fig. 6. Depletion of Nir2 in MDA-MB-231 cells substantially inhibits lung metastasis. (A,B) Control and Nir2-depleted MDA-MB-231 cells were injected intravenously (7.5×10^5 cells per mouse) into 5-week-old female SCID mice through the tail vein. Ten weeks later, lungs were removed from all mice (nine mice for each group) and fixed as described in Materials and Methods. The lung nodules were then counted and lung sections were prepared. Representative pictures of lungs from each group are shown (A). Quantitative evaluation of detectable nodules on the surface of the whole lungs is shown in B. Data are expressed as mean ± s.d. (*, $P<0.05$). (C) Representative histological photomicrographs of lung sections stained with H&E (2×). Arrowheads indicate tumor islands.

tumors stained positively for Nir2 ($P=0.029$, χ^2-statistics, Fig. 7D), indicating a correlation between high-grade, more aggressive tumors with poorer prognosis and Nir2 protein expression. Moreover, analysis of Nir2 expression and EMT markers in clinical breast cancer samples ($n=4467$) suggests that Nir2 expression adversely affects the prognosis of patients with an elevated EMT marker score (supplementary material Table S1; Fig. S3E,F). Samples that showed high expression of both Nir2 and EMT markers, as compared to those with only high expression of EMT markers, correlated with a statistically significant decreased survival of the patient. Collectively, our results suggest that high expression of Nir2 enhances EMT *in vitro*, facilitates cancer metastasis in animal models and correlates with poor prognosis of human patients.

DISCUSSION

Metastasis, the spreading of cancer cells from a primary tumor to seed secondary tumors in distant sites, is the main cause of mortality in breast cancer patients (Oppenheimer, 2006). Recent studies suggest that EMT plays a central role in motility and dissemination of cancer cells (Thiery et al., 2009). This dynamic and reversible process is necessary for efficient metastatic colonization (Brabletz, 2012) and is regulated by several signaling cascades that activate specific transcription factors (Huber et al., 2005).

In this study, we show that the PtdIns-transfer protein Nir2 potentiates EMT in mammary cells (Fig. 3) and is required for lung metastasis of breast cancer cells (Fig. 6). Remarkably, the expression level of Nir2 is upregulated in response to EMT inducers (Fig. 3A), such as EGF and TGFβ, and is markedly enhanced in human breast cancer tissue (Fig. 7). These results introduce Nir2 as a new positive regulator of EMT and breast cancer metastasis. Indeed, depletion of Nir2 by shRNA substantially inhibits cell migration and invasion, whereas its overexpression had opposite effects (Figs 1, 2 and Fig. 5B). Consistent with these results, previous studies have demonstrated that Nir2 expression is upregulated in invading endothelial cells grown in 3D collagen matrices as well as in mobile hematopoietic stem cells (Gan et al., 2008; Su et al., 2008). However, the underlying mechanisms of Nir2 function in these cells remain unknown.

Our studies suggest that Nir2 mediates its effects in mammary epithelial cells predominantly through the PI3K/AKT and the ERK signaling pathways (Fig. 1E and Fig. 2D; supplementary

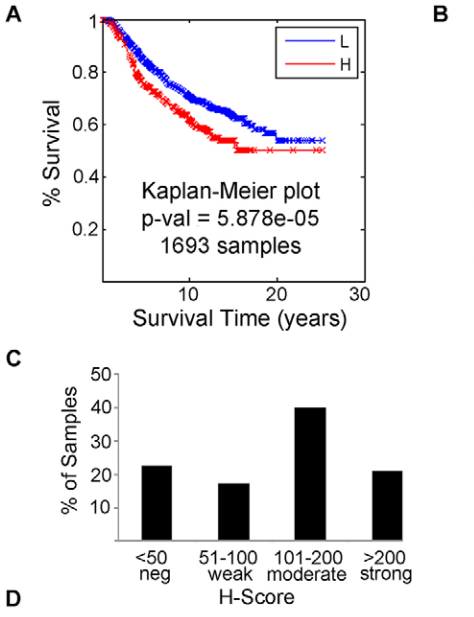

	Nir2 expression			
Tumor grade	*Total*	*Positive (%)*	*Negative (%)*	p-value
Low/Intermediate	28	18 (64)	10 (36)	0.029
High	22	20 (91)	2 (9)	

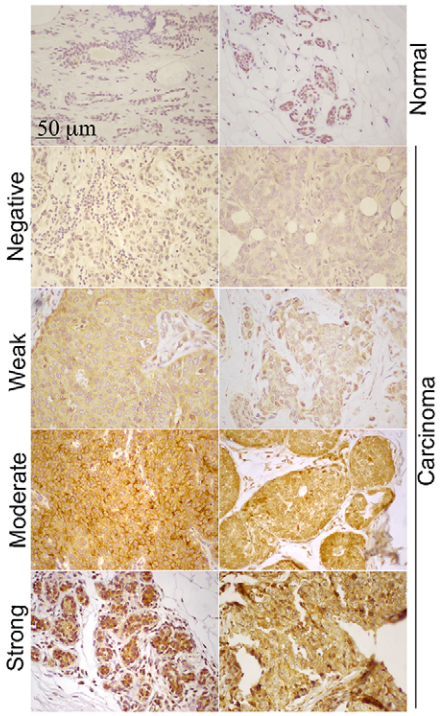

Fig. 7. Nir2 expression is upregulated in breast cancer tissues and is associated with poor patient prognosis. (A) Kaplan–Meier analysis was used to assess the overall survival of patients exhibiting low expression of Nir2 (blue line) and those exhibiting high Nir2 expression (red line). The analysis was performed on data derived from 1693 patients (Curtis et al., 2012), $P=5.878\times10^{-5}$. (B) Immunohistochemical analysis of Nir2 expression in normal mammary tissue and breast cancer samples. Representative pictures are shown. Staining intensity was classified as strong, moderate and weak. (C) Quantitative evaluation of 56 breast cancer patient samples using H-score (H-score$=\Sigma\ P_i$, (i+1), where P_i, is the percentage of stained cells in each intensity category, and i is the intensity for i=1, 2, 3). (D) Tumor samples were evaluated for tumor grade (supplementary material Table S2) and compared to Nir2 expression. Statistical analysis was performed by using χ^2-analysis.

Journal of Cell Science

Journal of Cell Science (2014) 127, 4740–4749 doi:10.1242/jcs.155721

material Figs S1D, S2B). These pathways contribute to all aspects of breast cancer progression, including cell growth, survival, migration, invasion and metastasis (Whyte et al., 2009; Pal and Mandal, 2012). Furthermore, the PI3K/AKT pathway is abnormally activated in about 30% of breast cancer patients (Cancer Genome Atlas Network, 2012), and is required for EMT. Specific inhibitors of the PI3K/AKT pathway, dominant-negative AKT or a Myr-AKT mutant markedly affect EMT in mammary cells (Bakin et al., 2000; Grille et al., 2003). We show here that Myr-AKT can rescue the effects of Nir2 depletion on the expression of vimentin and CD44 (Fig. 4), two characteristic EMT markers, thus demonstrting the central role of AKT activation in Nir2-mediated EMT effects. Interestingly, previous studies have shown that CD44s also enhances EMT through activation of AKT (Brown et al., 2011), suggesting a positive feedback during EMT.

The influence of Nir2 on PI3K/AKT and ERK signaling pathways is possibly related to its PtdIns-transfer activity and its effect on PtdIns(4,5)P_2 and PtdIns(3,4,5)P_3 production at the plasma membrane – as described in a recent publication of ours (Kim et al., 2013). Our findings were further supported by an independent study demonstrating that Nir2, through its PtdIns-transfer activity, promotes the replenishment of PtdIns(4,5)P_2 at the plasma membrane after receptor-induced PtdIns(4,5)P_2 hydrolysis (Chang et al., 2013). Both studies suggest that Nir2 influences PtdIns(4,5)P_2 levels through its plasma-membrane-associated pool, whereas its Golgi-associated pool possibly ensures efficient transport (Kim et al., 2013). In this context, it is important to mention that depletion of Nir2 by using shRNA in either MCF10A or MDA-MB-231 cells had no effect on Golgi-to-plasma membrane transport (supplementary material Fig. S4A).

Although Nir2 may influence cell migration and invasion through PtdIns-mediated pathways, we cannot exclude other mechanisms such as interaction with other cellular proteins. Consistent with this hypothesis, we have previously shown that Nir2 interacts with proteins that regulate cell migration and invasion, such as the small GTPase RhoA (Tian et al., 2002) and the tyrosine kinase PYK2 (Lev et al., 1999). Although we could not detect an association with either RhoA or PYK2 in these cells, we found Nir2 in focal adhesions after re-plating MDA-MB-231 cells on fibronection-coated coverslips (not shown). Thus, it could be that Nir2, through its multiple structural domains (Lev, 2004), can regulate different migratory events, such as actin organization, focal adhesion turnover and cell spreading. Indeed, depletion of Nir2 in MDA-MB-231 cells markedly affected the organization of the actin cytoskeleton and the formation of the leading edge (supplementary material Fig. S4B). Furthermore, recent studies suggest that VAPB, an integral ER-protein that interacts with Nir2 through a specific sequence motif known as FFAT (two phenylalanine residues in an acidic tract) (Amarilio et al., 2005), regulates the proliferation of breast tumor cells and activation of AKT (Rao et al., 2012). VAPB expression levels are also elevated in primary and metastatic breast cancer specimens, and correlate negatively with patient survival (Rao et al., 2012). Similarily, we show here that high expression of Nir2 correlates with poor prognosis and bad disease outcome (Fig. 7). Furthermore, depletion of Nir2 expression in MDA-MB-231 markedly reduced the number and size of lung metastases in a mice xenograft tail-vain-injection model. Although the tail-vain-injection model is commonly used to study lung metastasis of breast cancer (Rashid et al., 2013), it bypassess the early steps of the metaststic cascade, including local invasion and intravasation, and addresses late metastic events such as extravasion and local outhgrowth (Khanna and Hunter, 2005). We assume that Nir2 is involved in both early and late metaststic steps, as it markedly affects EMT-associated events (Figs 3, 5) that regulate early metastatic steps and also influences late events, as shown in Fig. 6.

Taken together, our results demonstrate for the first time that Nir2 is a regulator of EMT in breast cancer cells, and that Nir2 expression affects cell migration and invasion *in vitro*, lung metastasis in animal models and disease outcome in human patients. Further studies on Nir2 and its role in cell migration, invasion and metastasis could shed light on the mechanisms by which lipid-transfer proteins regulate key cellular processes and contribute to cancer metastasis.

MATERIALS AND METHODS

Cell culture

MCF10A cells were grown in DMEM:F12 (1:1) medium supplemented with EGF (10 ng/ml), insulin (10 µg/ml), cholera toxin (1 µg/ml), hydrocortisone (1 µg/ml) and heat-inactivated horse serum (5%). MDA-MB-231, T47D, SKBR3 and MDA-MB-468 cells were grown in RPMI (Gibco BRL; Grand Island, NY) medium supplemented with 10% fetal calf serum (FCS). Human embryonic kidney (HEK-293T) cells were grown in DMEM (Gibco BRL; Grand Island, NY) supplemented with 10% heat-inactivated fetal bovine serum (FBS) (Gibco BRL, Grand Island, NY), 1 mM sodium pyruvate and a penicillin-streptomycin mixture (100 units/ml; 0.1 mg/ml; Beit Haemek, Israel).

Antibodies and reagents

TGFβ and IGF-I were purchased from ProSpec (Israel), NRG1 was purchased from PeproTech (Israel). EGF, Hoechst 33342, U0126 and other chemicals were purchased from Sigma-Aldrich. Monoclonal antibodies against Myc, ERK1/2 and phosphorylated ERK1/2 (pERK1/2) were purchased from Santa Cruz Biotechnology (Santa Cruz, CA). Antibodies against AKT and phosphorylated AKT (pAKT T308 and pAKT S473) were purchased from Cell Signaling Technologies (Beverly, MA). Antibodies against fibronectin, CD44 and vimentin were purchased from Developmental Studies Hybridoma Bank (Iowa City, IA) Monoclonal antibodies against general vesicular transport factor p115 (USO1) as well as rabbit polyclonal antibodies against Nir2 have been described previously (Peretti et al., 2008). Goat polyclonal antibody against Nir2 was purchased from Abcam (Cambridge, UK). Monoclonal antibodies against α-tubulin and Rac1 were purchased from Sigma and BD (San Jose, California), respectively. Alexa-Fluor-488 donkey anti-mouse as well as anti-rabbit immunoglobulin Gs (IgGs) were purchased from Invitrogen (Carlsbad, CA). Cyanine (Cy)3-conjugated goat anti-rabbit and goat anti-mouse IgGs, as well as Cy5-conjugated goat anti-mouse IgG were purchased from Jackson ImmunoResearch Laboratories (West Grove, PA).

DNA constructs and lentivirus production and infection

Lentiviruses encoding shRNAs targeting Nir2 or Myc-tagged wild-type Nir2 (Nir2-Myc) have been described previously (Kim et al., 2013). Lentiviral vector encoding myristoylated (constitutively active) AKT (Myr-Akt) was established by subcloning the Myr-AKT cDNA from the pCIS2-AKT-Myr vector (kindly provided by Michael J. Quon, University of Maryland) into the PHAGE lentiviral vector. Lentivirus production and infection were conducted essentially as previously described (Kim et al., 2013). Infected MCF10A or T47D cells were grown in selection medium containing 100 µg/ml hygromycin, whereas MDA-MB-231 cells were grown in the presence of 400 µg/ml hygromycin for 72 hr.

Cell growth assay

The MTT [3-(4, 5-dimethylthiazolyl-2)-2,5-diphenyltetrazolium bromide] assay was used to measure the proliferation of MDA-MB-231 and MCF10A, essentially as previously described (Mosmann, 1983).

Immunofluorescence and confocal microscopy

Cells were grown on coverslips, washed with PBS and fixed, as described in the figure legends. To analyse localization of Nir2, cells grown on coverslips were fixed in 1% PFA in a hypotonic buffer (10 mM 2-(*N*-morpholino) ethanesulfonic acid pH 6.2, 10 mM NaCl, 1.5 mM $MgCl_2$ and 2.5% glycerol) for 20 min at room temperature and immunostained as described previously (Peretti et al., 2008). The cells were then incubated for 15 min in PBS containing 0.1 M glycine, incubated in blocking buffer containing 0.1% Triton X-100, 10% goat serum and 2% BSA in TBS for 30 min, followed by 1-hour incubation with the primary antibody, and 1-hour incubation with the secondary antibody. In specific experiments, coverslips were coated with 20 µg/ml of fibronectin for 16 hours at 4˚C. The specimens were analyzed by using a confocal laser scanning microscope (Zeiss 510; Carl Zeiss, Jena, Germany).

RNA extraction, RT-PCR and real-time PCR analysis

RNA was purified using the EZ-RNA kit (Beit Haemek, Israel). cDNA was generated using the SuperScriptII first-strand synthesis kit (Invitrogen; Carlsbad, CA). Reverse transcriptase (RT)-PCR was performed using Red-Taq mix (Sigma-Aldrich, Israel). Real-time PCR analysis was performed using SYBR Green I as a fluorescent dye, according to the manufacturer's guidelines (Invitrogen). All experiments were carried out in triplicates and normalized to actin RNA levels. Real-time PCR primers were designed using the Primerexpress software of Applied Biosystems (Invitrogen).

Gelatin zymography

To detect MMP2 and MMP9 activity, conditioned medium was separated electrophortically on 10% polyacrylamide/0.1% gelatin-embedded gels. The gels were then washed in 2.5% Triton X-100, and incubated at 37˚C for 24 hours in 50 mM Tris-HCl (pH 7.5), containing 0.2 M NaCl, 5 mM $CaCl_2$, 0.02% Brij 35, and stained using Coomassie Brilliant Blue (Pierce).

Wound-healing assays

Wound-healing assays were performed according to the manufacturer's protocol (iBidi, Germany). Briefly, cells were trypsinized and diluted in normal medium at 10^6 cells/ml and 70 µl were plated into each well, resulting in a confluent layer within 16 hr. Thereafter, the insert was removed and cells were allowed to migrate for different durations in the presence or absence of growth factor. Graphical presentation of the percentage of the wound healing was measured with the following formula: (initial width − time point width of wound) ÷ initial width of wound. The experiments were done in the presence of 10 µM mitomycin C to inhibit cell proliferation.

Transwell cell migration and invasion

Cells [MDA-MB-231 (45×10^3 cells/insert), MCF10A (50×10^3 cells/insert) and T47D (80×10^3 cells/insert)] were plated in the upper compartment of a Transwell tray (BD Bioscience, San Jose, California). For T47D cells, the lower compartment was coated with 25 ug/ml collagen for 2 h prior to cell plating. Cells were allowed to migrate through the intervening nitrocellulose membrane for 18 hr in the presence of growth factor in the lower chamber. Thereafter, cells were fixed in saline-containing paraformaldehyde (PFA; 3%), permeabilized in Triton X-100 (0.05%) and stained with Methyl Violet (0.02%). Non-migrating cells, growing on the upper side of the filter, were removed and cells that had migrated photographed. For cell invasion assays, 60×10^3 cells/insert (MDA-MB-231) or 80×10^3 cells/insert (MCF10A) were plated in the upper compartment of BioCoat Matrigel Chambers (BD Bioscience, San Jose, California) and processed as above.

Metastasis assays in animals

All animal procedures were carried out in accordance with the Guidelines for the Care and Use of Research Animals at the Weizmann Institute. Female CB-17 severe combined immunodeficient (SCID) mice were maintained and treated under specific pathogen-free conditions. Cells (7.5×10^5/mouse) were injected into the tail vein of 5-week-old female mice (15 mice/group). Ten weeks post injection, mice were sacrificed, the lungs were removed and fixed in Bouin solution for 24 hours. The lungs were imaged and nodules were counted. Representative slices were stained with hematoxylin and eosin (H&E). Statistical analyses used *t*-test.

Breast cancer sample analysis

Kaplan-Meyer analysis of the data from breast cancer samples (Curtis et al., 2012) was done using a software written by Assif Yitzhaky (The Weizmann Institute of Science).

Immunohistochemistry

Tissue samples of invasive breast cancer cases were obtained with institutional review board approval and informed consent from patients undergoing surgical resection at the Department of Gynecology and Obstetrics at the Goethe-University in Frankfurt am Main (Germany). Samples were characterized according standard pathology, including estrogen receptor, progesterone receptor and HER2 status. Formalin-fixed paraffin-embedded sections (3 µm) were mounted on Superfrost Plus slides. Immunohistochemistry was performed as follows; 3-µm serial sections from formalin-fixed, paraffin-embedded breast carcinoma were deparaffinized, rehydrated and pre-treated for antigen retrieval by microwave treatment for 10 min in 10 µM of citrate buffer pH 6.0. Samples were then incubated with goat anti-Nir2 antibody (Abcam) overnight at RT. Biotinylated rabbit anti-goat antiserum (DakoCytomation) served as secondary antibody. Strept/AB was used according to the manufacturer's protocol (DakoCytomation). After rinsing with phosphate buffer, sections were counterstained with DAB (Merck), dehydrated and mounted on coverslips.

Scoring of tissue samples

Samples from 56 breast cancer patients and from seven healthy individuals were stained. The intensity of specific staining was characterized as not present (0), weak (1+), moderate (2+) and strong (3+). For each sample, a summary value, referred to as H-Score, was calculated (Kraus et al., 2012). This consists of the sum of the percentages of positively stained cells multiplied by a weighted intensity of staining. H-Score$=\Sigma\ P_i$, (i+1), where P_i, is the percentage of stained cells in each intensity category, and i is the intensity for i=0, 1, 2, 3. Tumor grade was evaluated according clinical and pathological data (supplementary material Table S2). Statistics were performed using χ^2-analysis.

Densitometry and statistical analysis

The densitometric analysis of western blot bands was determined using NIH ImageJ software. Results are presented as means ± s.d. Differences between experimental conditions were determined by two-tailed Student's *t* test. $*P<0.05$, $**P<0.01$ and $***P<0.001$ denote statistical relevance.

Acknowledgements

S.L. is the incumbent of the Joyce and Ben B. Eisenberg Chair of Molecular Biology and Cancer Research. We thank Assif Yitzhaky and Dvir Netanely for bioinformatics assistance and Nir Ben-Chetrit for excellent suggestions.

Competing interests

The authors declare no competing interests.

Author contributions

O.K. and A.K. designed and performed the experiments reported in Figs 1-5. N.G. participated in the in vivo assay (Fig. 6) and carried out the IHC analysis reported in Fig. 7. M.S. and S.K. prepared reagents. S.B. acquired the surgical breast cancer patient samples. T.K. analyzed and accumulated the patient data reported in supplementary material Fig. S3E,F. S.L. designed the study and wrote the manuscript. All authors read and approved the final manuscript.

Funding

This work was supported by the Israel Science Foundation (ISF) [grant No. 1223/12], the Israel Cancer Association, and the Jeanne and Joseph Nissim Foundation for Life Sciences Research.

Supplementary material

Supplementary material available online at
http://jcs.biologists.org/lookup/suppl/doi:10.1242/jcs.155721/-/DC1

References

Amarilio, R., Ramachandran, S., Sabanay, H. and Lev, S. (2005). Differential regulation of endoplasmic reticulum structure through VAP-Nir protein interaction. *J. Biol. Chem.* **280**, 5934-5944.

Bakin, A. V., Tomlinson, A. K., Bhowmick, N. A., Moses, H. L. and Arteaga, C. L. (2000). Phosphatidylinositol 3-kinase function is required for transforming growth factor beta-mediated epithelial to mesenchymal transition and cell migration. *J. Biol. Chem.* **275**, 36803-36810.

Bartucci, M., Morelli, C., Mauro, L., Andò, S. and Surmacz, E. (2001). Differential insulin-like growth factor I receptor signaling and function in estrogen receptor (ER)-positive MCF-7 and ER-negative MDA-MB-231 breast cancer cells. *Cancer Res.* **61**, 6747-6754.

Batlle, E., Sancho, E., Francí, C., Domínguez, D., Monfar, M., Baulida, J. and García De Herreros, A. (2000). The transcription factor snail is a repressor of E-cadherin gene expression in epithelial tumour cells. *Nat. Cell Biol.* **2**, 84-89.

Bellacosa, A. L. L. (2010). PI3K/AKT pathway and the epithelial-mesenchymal transition. In *Cancer Genome and Tumor Microenvironment* (ed. T. Tikhonenko-Andrei), pp. 11-21. New York, NY: Springer.

Bolós, V., Peinado, H., Pérez-Moreno, M. A., Fraga, M. F., Esteller, M. and Cano, A. (2003). The transcription factor Slug represses E-cadherin expression and induces epithelial to mesenchymal transitions: a comparison with Snail and E47 repressors. *J. Cell Sci.* **116**, 499-511.

Brabletz, T. (2012). EMT and MET in metastasis: where are the cancer stem cells? *Cancer Cell* **22**, 699-701.

Brown, R. L., Reinke, L. M., Damerow, M. S., Perez, D., Chodosh, L. A., Yang, J. and Cheng, C. (2011). CD44 splice isoform switching in human and mouse epithelium is essential for epithelial-mesenchymal transition and breast cancer progression. *J. Clin. Invest.* **121**, 1064-1074.

Cancer Genome Atlas Network (2012). Comprehensive molecular portraits of human breast tumours. *Nature* **490**, 61-70.

Chang, C. L., Hsieh, T. S., Yang, T. T., Rothberg, K. G., Azizoglu, D. B., Volk, E., Liao, J. C. and Liou, J. (2013). Feedback regulation of receptor-induced Ca2+ signaling mediated by E-Syt1 and Nir2 at endoplasmic reticulum-plasma membrane junctions. *Cell Reports* **5**, 813-825.

Cho, S. J., Chae, M. J., Shin, B. K., Kim, H. K. and Kim, A. (2008). Akt- and MAPK-mediated activation and secretion of MMP-9 into stroma in breast cancer cells upon heregulin treatment. *Mol. Med. Rep.* **1**, 83-88.

Curtis, C., Shah, S. P., Chin, S. F., Turashvili, G., Rueda, O. M., Dunning, M. J., Speed, D., Lynch, A. G., Samarajiwa, S., Yuan, Y. et al.; METABRIC Group (2012). The genomic and transcriptomic architecture of 2,000 breast tumours reveals novel subgroups. *Nature* **486**, 346-352.

Gan, B., Sahin, E., Jiang, S., Sanchez-Aguilera, A., Scott, K. L., Chin, L., Williams, D. A., Kwiatkowski, D. J. and DePinho, R. A. (2008). mTORC1-dependent and -independent regulation of stem cell renewal, differentiation, and mobilization. *Proc. Natl. Acad. Sci. USA* **105**, 19384-19389.

Grille, S. J., Bellacosa, A., Upson, J., Klein-Szanto, A. J., van Roy, F., Lee-Kwon, W., Donowitz, M., Tsichlis, P. N. and Larue, L. (2003). The protein kinase Akt induces epithelial mesenchymal transition and promotes enhanced motility and invasiveness of squamous cell carcinoma lines. *Cancer Res.* **63**, 2172-2178.

Gupta, G. P. and Massagué, J. (2006). Cancer metastasis: building a framework. *Cell* **127**, 679-695.

Hardy, K. M., Booth, B. W., Hendrix, M. J., Salomon, D. S. and Strizzi, L. (2010). ErbB/EGF signaling and EMT in mammary development and breast cancer. *J. Mammary Gland Biol. Neoplasia* **15**, 191-199.

Harrison, S. M., Knifley, T., Chen, M. and O'Connor, K. L. (2013). LPA, HGF, and EGF utilize distinct combinations of signaling pathways to promote migration and invasion of MDA-MB-231 breast carcinoma cells. *BMC Cancer* **13**, 501.

Hollestelle, A., Elstrodt, F., Nagel, J. H., Kallemeijn, W. W. and Schutte, M. (2007). Phosphatidylinositol-3-OH kinase or RAS pathway mutations in human breast cancer cell lines. *Mol. Cancer Res.* **5**, 195-201.

Huber, M. A., Kraut, N. and Beug, H. (2005). Molecular requirements for epithelial-mesenchymal transition during tumor progression. *Curr. Opin. Cell Biol.* **17**, 548-558.

Imamura, T., Hikita, A. and Inoue, Y. (2012). The roles of TGF-β signaling in carcinogenesis and breast cancer metastasis. *Breast Cancer* **19**, 118-124.

Irie, H. Y., Pearline, R. V., Grueneberg, D., Hsia, M., Ravichandran, P., Kothari, N., Natesan, S. and Brugge, J. S. (2005). Distinct roles of Akt1 and Akt2 in regulating cell migration and epithelial-mesenchymal transition. *J. Cell Biol.* **171**, 1023-1034.

Iwatsuki, M., Mimori, K., Yokobori, T., Ishi, H., Beppu, T., Nakamori, S., Baba, H. and Mori, M. (2010). Epithelial-mesenchymal transition in cancer development and its clinical significance. *Cancer Sci.* **101**, 293-299.

Khanna, C. and Hunter, K. (2005). Modeling metastasis in vivo. *Carcinogenesis* **26**, 513-523.

Kim, E. S., Kim, M. S. and Moon, A. (2004). TGF-beta-induced upregulation of MMP-2 and MMP-9 depends on p38 MAPK, but not ERK signaling in MCF10A human breast epithelial cells. *Int. J. Oncol.* **25**, 1375-1382.

Kim, S., Kedan, A., Marom, M., Gavert, N., Keinan, O., Selitrennik, M., Laufman, O. and Lev, S. (2013). The phosphatidylinositol-transfer protein Nir2 binds phosphatidic acid and positively regulates phosphoinositide signalling. *EMBO Rep.* **14**, 891-899.

Köhrmann, A., Kammerer, U., Kapp, M., Dietl, J. and Anacker, J. (2009). Expression of matrix metalloproteinases (MMPs) in primary human breast cancer and breast cancer cell lines: new findings and review of the literature. *BMC Cancer* **9**, 188.

Kraus, J. A., Dabbs, D. J., Beriwal, S. and Bhargava, R. (2012). Semi-quantitative immunohistochemical assay versus oncotype DX((R)) qRT-PCR assay for estrogen and progesterone receptors: an independent quality assurance study. *Mod. Pathol.* **25**, 869-876.

Lee, T. K., Poon, R. T., Yuen, A. P., Ling, M. T., Kwok, W. K., Wang, X. H., Wong, Y. C., Guan, X. Y., Man, K., Chau, K. L. et al. (2006). Twist overexpression correlates with hepatocellular carcinoma metastasis through induction of epithelial-mesenchymal transition. *Clin. Can. Res.* **12**, 5369-5376.

Lev, S. (2004). The role of the Nir/rdgB protein family in membrane trafficking and cytoskeleton remodeling. *Exp. Cell Res.* **297**, 1-10.

Lev, S., Hernandez, J., Martinez, R., Chen, A., Plowman, G. and Schlessinger, J. (1999). Identification of a novel family of targets of PYK2 related to Drosophila retinal degeneration B (rdgB) protein. *Mol. Cell. Biol.* **19**, 2278-2288.

Litvak, V., Dahan, N., Ramachandran, S., Sabanay, H. and Lev, S. (2005). Maintenance of the diacylglycerol level in the Golgi apparatus by the Nir2 protein is critical for Golgi secretory function. *Nat. Cell Biol.* **7**, 225-234.

Lo, H. W., Hsu, S. C., Xia, W., Cao, X., Shih, J. Y., Wei, Y., Abbruzzese, J. L., Hortobagyi, G. N. and Hung, M. C. (2007). Epidermal growth factor receptor cooperates with signal transducer and activator of transcription 3 to induce epithelial-mesenchymal transition in cancer cells via up-regulation of TWIST gene expression. *Cancer Res.* **67**, 9066-9076.

Mosmann, T. (1983). Rapid colorimetric assay for cellular growth and survival: application to proliferation and cytotoxicity assays. *J. Immunol. Methods* **65**, 55-63.

Oppenheimer, S. B. (2006). Cellular basis of cancer metastasis: a review of fundamentals and new advances. *Acta Histochem.* **108**, 327-334.

Pal, I. and Mandal, M. (2012). PI3K and Akt as molecular targets for cancer therapy: current clinical outcomes. *Acta Pharmacol. Sin.* **33**, 1441-1458.

Peretti, D., Dahan, N., Shimoni, E., Hirschberg, K. and Lev, S. (2008). Coordinated lipid transfer between the endoplasmic reticulum and the Golgi complex requires the VAP proteins and is essential for Golgi-mediated transport. *Mol. Biol. Cell* **19**, 3871-3884.

Price, J. T., Tiganis, T., Agarwal, A., Djakiew, D. and Thompson, E. W. (1999). Epidermal growth factor promotes MDA-MB-231 breast cancer cell migration through a phosphatidylinositol 3′-kinase and phospholipase C-dependent mechanism. *Cancer Res.* **59**, 5475-5478.

Rao, M., Song, W., Jiang, A., Shyr, Y., Lev, S., Greenstein, D., Brantley-Sieders, D. and Chen, J. (2012). VAMP-associated protein B (VAPB) promotes breast tumor growth by modulation of Akt activity. *PLoS ONE* **7**, e46281.

Rashid, O. M., Nagahashi, M., Ramachandran, S., Dumur, C. I., Schaum, J. C., Yamada, A., Aoyagi, T., Milstien, S., Spiegel, S. and Takabe, K. (2013). Is tail vein injection a relevant breast cancer lung metastasis model? *J. Thorac. Dis.* **5**, 385-392.

Romagnoli, M., Belguise, K., Yu, Z., Wang, X., Landesman-Bollag, E., Seldin, D. C., Chalbos, D., Barillé-Nion, S., Jézéquel, P., Seldin, M. L. et al. (2012). Epithelial-to-mesenchymal transition induced by TGF-β1 is mediated by Blimp-1-dependent repression of BMP-5. *Cancer Res.* **72**, 6268-6278.

Savagner, P. (2001). Leaving the neighborhood: molecular mechanisms involved during epithelial-mesenchymal transition. *BioEssays* **23**, 912-923.

Savagner, P. (2010). The epithelial-mesenchymal transition (EMT) phenomenon. *Ann. Oncol.* **21 Suppl. 7**, vii89-92.

Somiari, S. B., Somiari, R. I., Heckman, C. M., Olsen, C. H., Jordan, R. M., Russell, S. J. and Shriver, C. D. (2006). Circulating MMP2 and MMP9 in breast cancer – potential role in classification of patients into low risk, high risk, benign disease and breast cancer categories. *Int. J. Cancer* **119**, 1403-1411.

Su, S. C., Mendoza, E. A., Kwak, H. I. and Bayless, K. J. (2008). Molecular profile of endothelial invasion of three-dimensional collagen matrices: insights into angiogenic sprout induction in wound healing. *Am. J. Physiol.* **295**, C1215-C1229.

Tarcic, G., Avraham, R., Pines, G., Amit, I., Shay, T., Lu, Y., Zwang, Y., Katz, M., Ben-Chetrit, N., Jacob-Hirsch, J. et al. (2012). EGR1 and the ERK-ERF axis drive mammary cell migration in response to EGF. *FASEB J.* **26**, 1582-1592.

Têtu, B., Brisson, J., Wang, C. S., Lapointe, H., Beaudry, G., Blanchette, C. and Trudel, D. (2006). The influence of MMP-14, TIMP-2 and MMP-2 expression on breast cancer prognosis. *Breast Cancer Research* **8**, R28.

Thiery, J. P. (2002). Epithelial-mesenchymal transitions in tumour progression. *Nat. Rev. Cancer* **2**, 442-454.

Thiery, J. P. and Sleeman, J. P. (2006). Complex networks orchestrate epithelial-mesenchymal transitions. *Nat. Rev. Mol. Cell Biol.* **7**, 131-142.

Thiery, J. P., Acloque, H., Huang, R. Y. and Nieto, M. A. (2009). Epithelial-mesenchymal transitions in development and disease. *Cell* **139**, 871-890.

Tian, D., Litvak, V., Toledo-Rodriguez, M., Carmon, S. and Lev, S. (2002). Nir2, a novel regulator of cell morphogenesis. *Mol. Cell. Biol.* **22**, 2650-2662.

Tsai, M. S., Shamon-Taylor, L. A., Mehmi, I., Tang, C. K. and Lupu, R. (2003). Blockage of heregulin expression inhibits tumorigenicity and metastasis of breast cancer. *Oncogene* **22**, 761-768.

Tumbarello, D. A. and Turner, C. E. (2007). Hic-5 contributes to epithelial-mesenchymal transformation through a RhoA/ROCK-dependent pathway. *J. Cell. Physiol.* **211**, 736-747.

Whyte, J., Bergin, O., Bianchi, A., McNally, S. and Martin, F. (2009). Key signalling nodes in mammary gland development and cancer. Mitogen-activated protein kinase signalling in experimental models of breast cancer progression and in mammary gland development. *Breast Cancer Research* **11**, 209.

Xiao, D. and He, J. (2010). Epithelial mesenchymal transition and lung cancer. *J. Thorac. Dis.* **2**, 154-159.

Figure S1

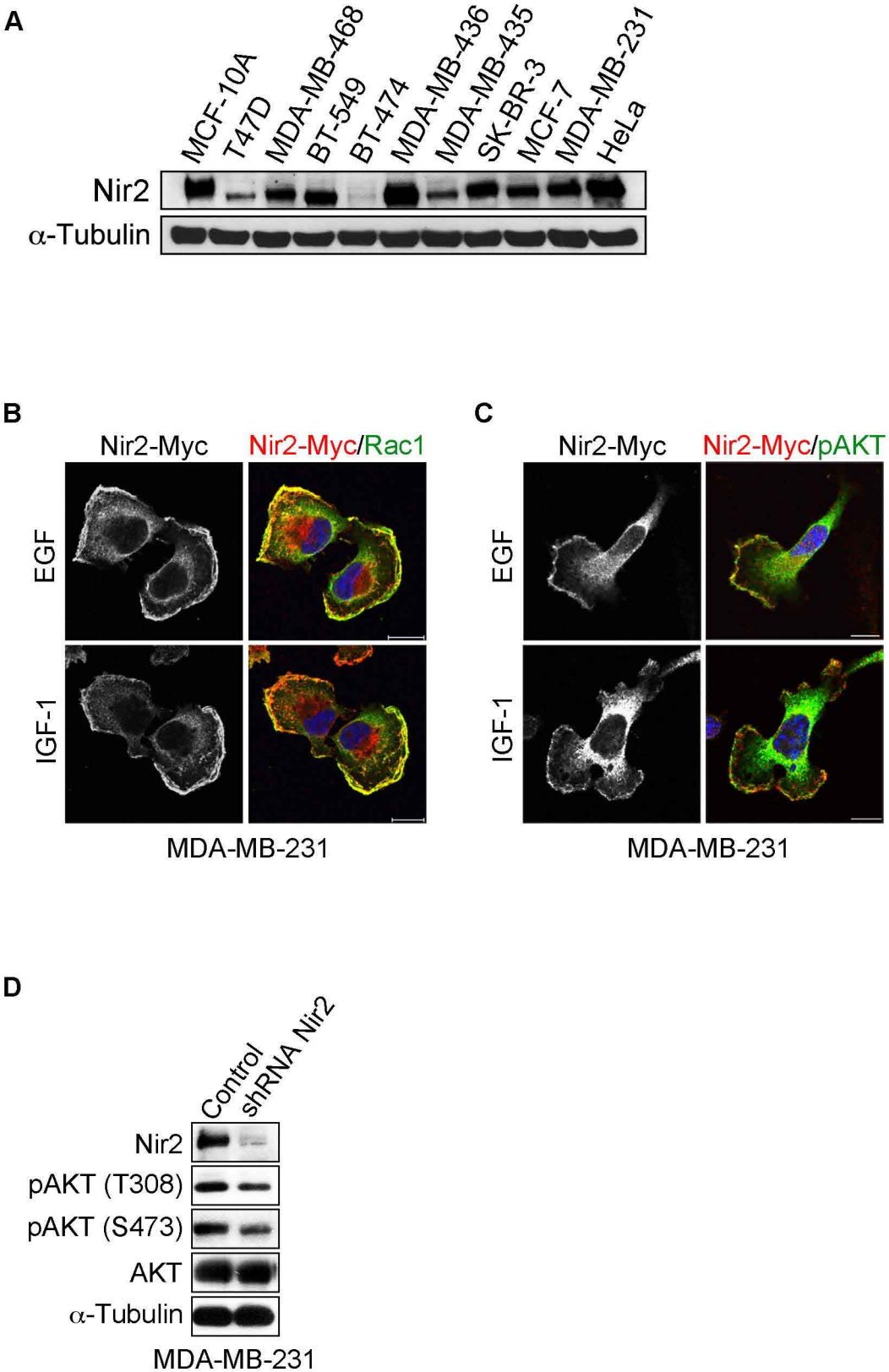
A
MCF-10A
T47D
MDA-MB-468
BT-549
BT-474
MDA-MB-436
MDA-MB-435
SK-BR-3
MCF-7
MDA-MB-231
HeLa
Nir2
α-Tubulin
B
Nir2-Myc
Nir2-Myc/Rac1
EGF
IGF-1
MDA-MB-231
C
Nir2-Myc
Nir2-Myc/pAKT
EGF
IGF-1
MDA-MB-231
D
Control
shRNA Nir2
Nir2
pAKT (T308)
pAKT (S473)
AKT
α-Tubulin
MDA-MB-231

Figure S2

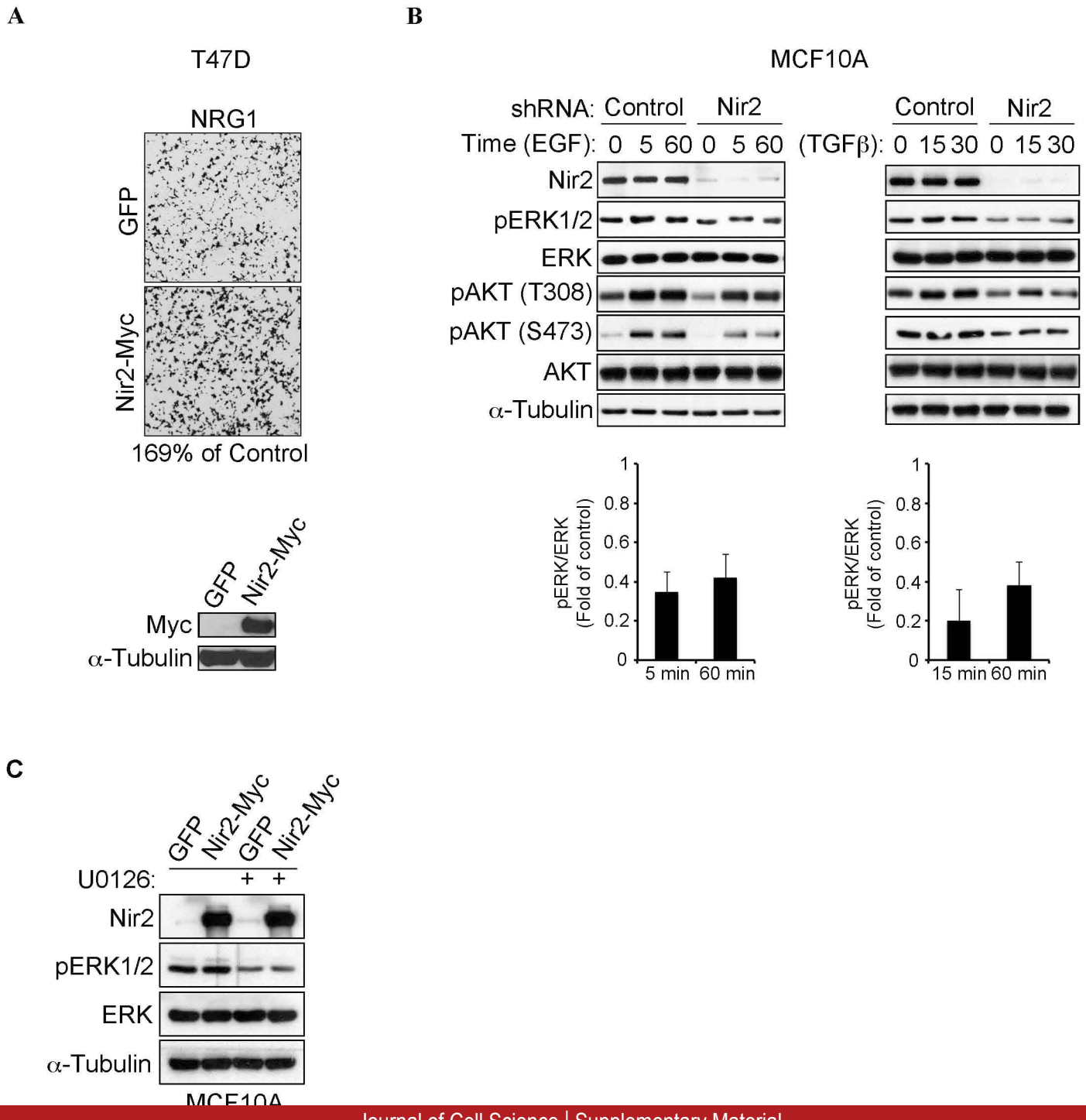
A
T47D
NRG1
GFP
Nir2-Myc
169% of Control
GFP
Nir2-Myc
Myc
α-Tubulin
B
MCF10A
shRNA: Control Nir2
Time (EGF): 0 5 60 0 5 60
Control Nir2
(TGFβ): 0 15 30 0 15 30
Nir2
pERK1/2
ERK
pAKT (T308)
pAKT (S473)
AKT
α-Tubulin
pERK/ERK (Fold of control)
5 min 60 min
15 min 60 min
C
GFP
Nir2-Myc
GFP
Nir2-Myc
U0126: + +
Nir2
pERK1/2
ERK
α-Tubulin
MCF10A

Figure S3

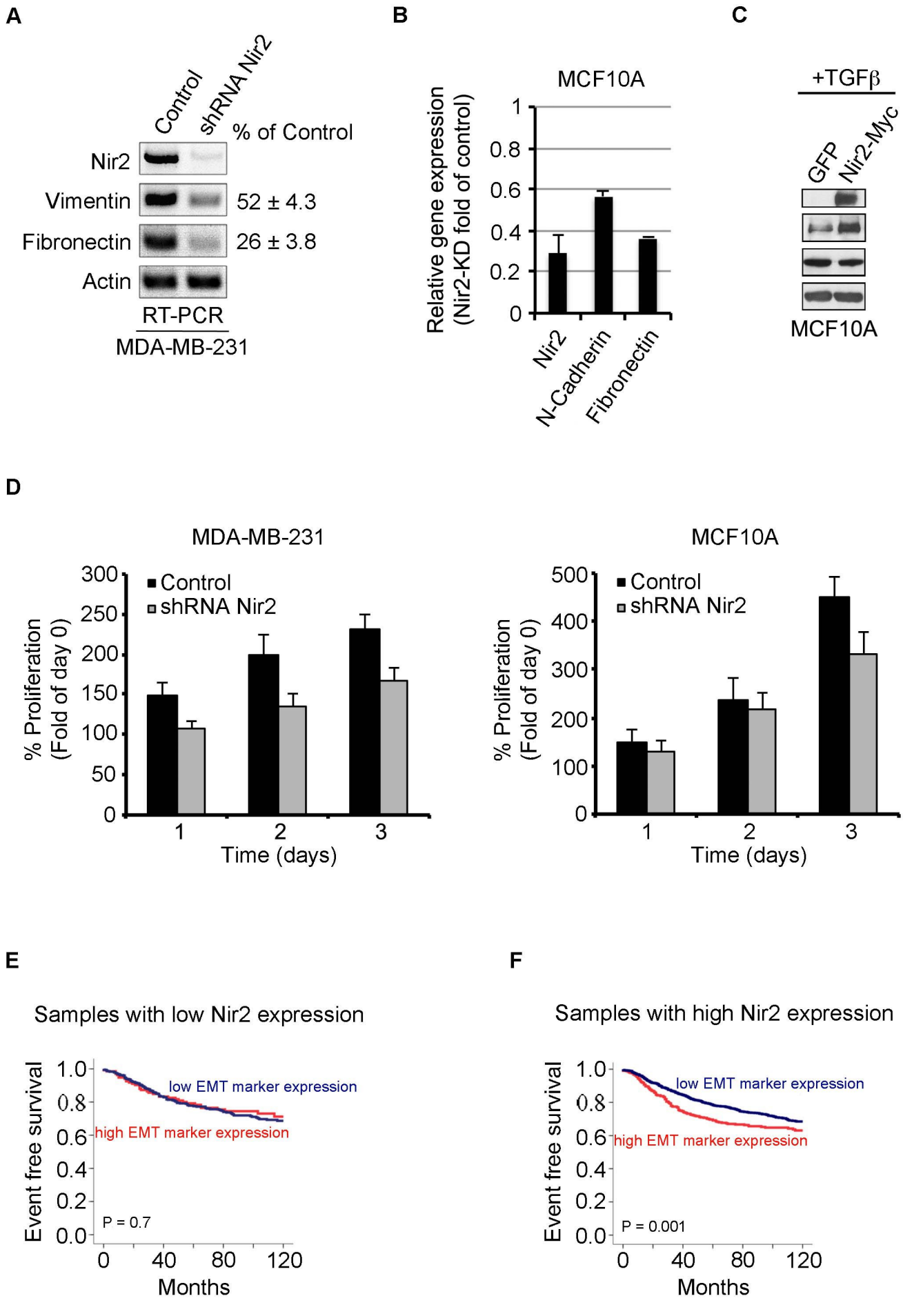
A
Control
shRNA Nir2
% of Control
Nir2
Vimentin
52 ± 4.3
Fibronectin
26 ± 3.8
Actin
RT-PCR
MDA-MB-231
B
MCF10A
Relative gene expression
(Nir2-KD fold of control)
1
0.8
0.6
0.4
0.2
0
Nir2
N-Cadherin
Fibronectin
C
+TGFβ
GFP
Nir2-Myc
MCF10A
D
MDA-MB-231
% Proliferation
(Fold of day 0)
300
250
200
150
100
50
0
Control
shRNA Nir2
1
2
3
Time (days)
MCF10A
% Proliferation
(Fold of day 0)
500
400
300
200
100
0
Control
shRNA Nir2
1
2
3
Time (days)
E
Samples with low Nir2 expression
Event free survival
1.0
0.8
0.6
0.4
0.2
0.0
low EMT marker expression
high EMT marker expression
P = 0.7
0
40
80
120
Months
F
Samples with high Nir2 expression
Event free survival
1.0
0.8
0.6
0.4
0.2
0.0
low EMT marker expression
high EMT marker expression
P = 0.001
0
40
80
120
Months

Figure S4

A

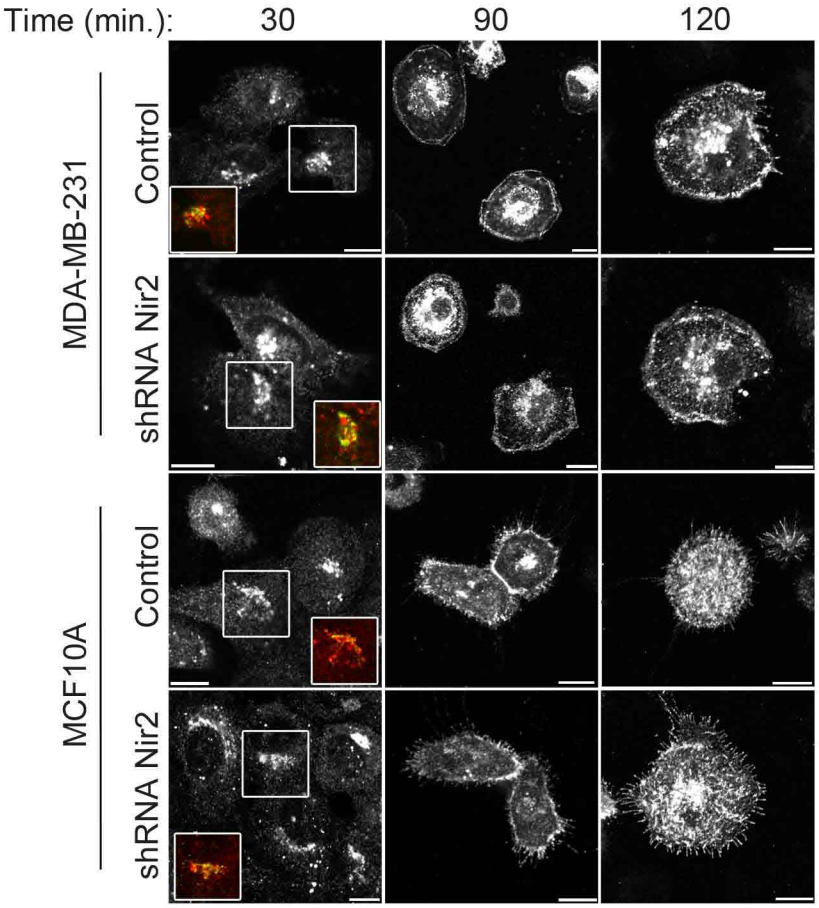
Time (min.):
30
90
120
MDA-MB-231
Control
shRNA Nir2
MCF10A
Control
shRNA Nir2

B

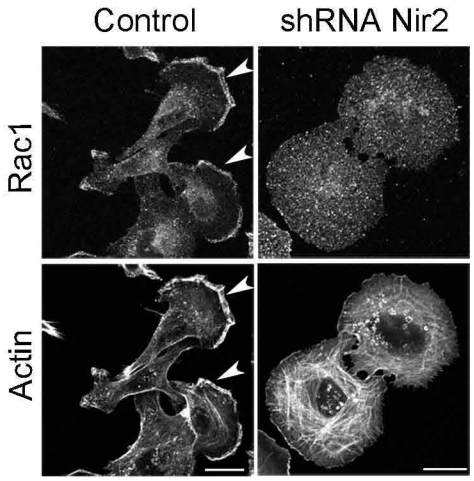
Control
shRNA Nir2
Rac1
Actin

Supplementary Information

Figure S1: **Nir2 is differentially expressed in human breast cancer cell lines, affects the activation of AKT, and localizes to the PM following GF treatment.** (A) The steady-state expression level of Nir2 in the indicated human cell lines was assessed by Western blotting (WB) of total cell lysates using anti-Nir2 antibody. WB with α-tubulin was used as a loading control. (B,C) MDA-MB-231 expressing Nir2-Myc were serum-starved for 16 hrs and then treated with EGF (50 ng/ml) or IGF-I (20 ng/ml) for 15 min at 37°C. The cells were then fixed and processed for immunofluorescence analysis using anti-Myc and either anti-Rac1 (A) or anti-pAKT (S473) (B) antibodies. Shown are representative confocal images. Co-localization of Nir2 and Rac1 or pAKT appears in yellow. Scale bar, 10 μm. (D) Control and Nir2-depleted MDA-MB-231 cells were grown in full medium. Total cell lysates were prepared and analyzed for AKT phosphorylation using the corresponding antibodies and Western blot analysis. Reproducible results were obtained in three independent experiments.

Figure S2: **Nir2 overexpression facilitates the migration of T47D cells, while Nir2 depletion attenuates ERK activation in MCF10A cells.** (A) T47D cells expressing either GFP or Nir2-Myc were plated in Boyden chambers and stimulated with NRG1 (20 ng/ml) for 24 hr. Cell migration was assessed as described in materials and methods. The mean values ±s.d. of three independent experiments are shown. (B) Nir2-depleted MCF10A cells were serum-starved for 24 hrs, and then stimulated with EGF (10 ng/ml) or TGFβ (5 ng/ml) for the indicated time periods. Total cell lysates were prepared and analyzed for ERK1/2 and AKT phosphorylation using Western blotting. The mean values ±s.d. of four independent experiments are shown. (C) MCF10A cells expressing either GFP or Nir2-Myc were grown in the absence or presence of the MEK1/2 inhibitor U0126 (1 μM) for 24 hours. Total cell lysates were prepared and analyzed for ERK1/2 and AKT phosphorylation using the corresponding antibodies and Western blotting.

Figure S3: **Nir2 influences proliferation and mRNA expression levels of EMT markers in MDA-MB-231 and MCF10A cells as well as the prognostic values of EMT markers in clinical breast cancer.** The mRNA levels of the indicated EMT markers were assessed in control and Nir2-depleted MDA-MB-231 cells (A) and MCF10A cells (B) by RT-PCR and real-time PCR, respectively. The mean values ±s.d. of four independent experiments are shown. (C) The influence of Nir2 overexpression on TGFβ (5 ng/ml for 3 days)-induced EMT markers was examined by WB using the indicated antibodies. (D) Control and Nir2-depleted MCF10A ($3*10^3$ cells/well) or MDA-MB-231 ($5*10^3$ cells/well) cells were seeded in 96 well plates and grown for the indicated time periods in a complete media. Cell viability was assessed by MTT assay. The relative MTT values obtained compared to zero time are shown. The mean values ±s.d. of three independent experiments are shown. (E,F) The prognostic value of an EMT marker score was calculated for 4,467 breast cancer samples with Affymetrix gene expression data that has been described previously (Hanker et al., 2013). The EMT marker score was based on the mean expression of 21 Affymetrix probesets representing a set of genes previously described to be upregulated during EMT (Table S1, (Hatami et al., 2013). Samples were then stratified using the highest quartile of this score as either high or low EMT marker expression. Two separate Kaplan-Meier analyses of event free survival of patients are shown either for those samples with low Nir2 expression (Affymetrix probeset 203826_s_at, lower quartile) in (E) or high Nir2 expression in (F).

Figure S4: Nir2 expression affects the spreading and polarization of MDA-MB-231 but not Golgi-to-plasma membrane transport of VSVG. (A) Control and Nir2-depleted MDA-MB-231 cells were plated on fibronectin coated coverslips and immunostained with anti-Rac1 antibody and TRITC-Phalloidin. Scale bar, 10 μm. (B) The VSVG transport assay was carried out as previously described (Kim et al., 2013). Shown are representative images of control and Nir2-depleted MDA-MB-231 and MCF10A cells at the indicated time points. Insert shows colocalization of VSVG and the Golgi marker GRASP65. Scale bar, 10μm.

References

Hanker, L. C., Rody, A., Holtrich, U., Pusztai, L., Ruckhaeberle, E., Liedtke, C., Ahr, A., Heinrich, T. M., Sanger, N., Becker, S. et al. (2013). Prognostic evaluation of the B cell/IL-8 metagene in different intrinsic breast cancer subtypes. *Breast cancer research and treatment* **137**, 407-416.

Hatami, R., Sieuwerts, A. M., Izadmehr, S., Yao, Z., Qiao, R. F., Papa, L., Look, M. P., Smid, M., Ohlssen, J., Levine, A. C. et al. (2013). KLF6-SV1 drives breast cancer metastasis and is associated with poor survival. *Science translational medicine* **5**, 169ra112.

Kim, S., Kedan, A., Marom, M., Gavert, N., Keinan, O., Selitrennik, M., Laufman, O. and Lev, S. (2013). The phosphatidylinositol-transfer protein Nir2 binds phosphatidic acid and positively regulates phosphoinositide signalling. *EMBO Rep* **14**, 891-899.

Table S1. The 21 probesets of marker genes that are upregulated during EMT.

Gene symbol	Affymetrix probeset
BMP1	202701_at
CDH2	203440_at
COL1A2	202403_s_at
FN1	210495_x_at
FOXC1	213260_at
GNG11	204115_at
ITGA5	201389_at
ITGAV	202351_at
MMP2	201069_at
MMP3	205828_at
MMP9	203936_s_at
MSN	200600_at
SNAI1	219480_at
SNAI2	213139_at
TCF4	213891_s_at
TGFB1	203085_s_at
TWIST1	213943_at
VCAN	221731_x_at
VIM	201426_s_at
ZEB1	212758_s_at
ZEB2	203603_s_at

A set of marker genes that are upregulated during EMT as previously described (Hatami et al., 2013) and for which probesets are available on Affymetrix U133A Gene-Chips. These 21 probesets were used to develop a robust EMT marker score. The relationship of Nir2 expression and the EMT marker score was assessed as described in Fig. S7.

Table S2. Correlation of Nir2 expression with clinical/pathologic parameters and other biomarkers.

	Nir2 expression			
Parameters/markers	*Total*	*Positive (%)*	*Negative (%)*	*P-value*
Age (years)				
<50	17	12 (71)	5 (29)	0.47
>50	39	31 (79)	8 (21)	
Tumor size				
<2 cm (T1)	27	18 (67)	9 (33)	0.096
>2 cm (T2,3,4)	28	24 (86)	4 (14)	
Lymph node status				
Negative	40	29 (72.5)	11 (27.5)	0.25
Positive	16	14 (87.5)	2 (12.5)	
Distant metastasis				
Positive	0			N/A
Negative	53	40 (75)	13 (25)	
ER status				
Positive	27	19 (70)	8 (30)	0.27
Negative	29	24 (83)	5 (17)	
PR status				
Positive	22	16 (73)	6 (27)	0.42
Negative	33	27 (82)	6 (18)	
HER-2/neu status				
Positive	9	8 (89)	1 (11)	0.33
Negative	46	34 (74)	12 (26)	
Subtype				
TNBC	23	18 (78)	5 (22)	0.83
Luminal/Her2+	33	25 (76)	8 (24)	

Correlation of Nir2 expression with clinical and pathologic parameters and other biomarkers. We found no statistical correlation between patient age, tumor size, lymph node status or biomarkers. However there was a statistically significant correlation between Nir2 expression and tumor grade (see Fig. 7D).